TR/11/81 November 1981

A numerical study of heat flow in an elliptic cylinder with interior derivative boundary conditions

E.H. Twizell
and
P. Smith*

Department of Mathematics and Computer Studies,
Sunderland Polytechnic, Sunderland. SRI 3SD

O . ABSTRACT

A three dimensional, time dependent study of heat flow in an elliptic cylinder is developed in this paper. Such a study is required in the computation of temperature distribution in segments of the human body, in particular the torso. The study is therefore developed in relation to the flow of heat in the human torso.The geometry of the torso is approximated by an elliptic cylinder of core surrounded longitudinally by an annulus of muscle and then surrounded totally by insulating layers of fat and skin.

The parabolic partial differential equation governing the flow of heat, together with the derivative boundary conditions between the four types of tissue and between the skin and the environment, and together with the initial conditions, is solved by a stable, implicit finite difference method based on the (1,0) Padé approximant to the exponential function The method is extrapolated in time to improve accuracy.

The formulation allows the environmental temperature to change with all three space variables and is seen to deal satisfactorily with the discontinuities in temperature which arise with instantaneous changes in environmental temperature.

The study is validated by duplicating a laboratory experiment carried out under extreme environmental conditions by the US Air Force, the numerical results showing an improvement on those obtained using a mathematical formulation developed by *NASA*. The study is further tested on a econd, related numerical experiment.

1. INTRODUCTION

The mathematical modelling of heat flow in the torso, and in other segments of the human body, has a number of important areas of application. The modelling of heat flow in the body in an industrial environment has been carried out in the United States by Fan, Hsu, Hwang, Konz *et al* at the Institute for Systems Design and Optimization at Kansas State University and in Great Britain by Thomas, Spencer and Davies at Politechnig Cymru, UWIST and the University of Birmingham [14]. Arguably one of the most important applications of the modelling of heat flow in the human body is in the analysis of physiological and bioengineering problems encountered in extravehicular Space Shuttle and *in lunâ* activities. Such research has been carried out extensively at, for example, NASA's Lyndon B. Johnson Space Center . to aid in the design and understanding of liquid cooled garments, the study of human thermal stress, and the study of performance under conditions of strenuous exercise in extreme environments (Kuznetz [6]).

Periodically, review papers are published on the modelling of heat flow in the human body ; these have included a review of mathematical models by Fan *et al* [1] and a review of engineering models by Hwang and Konz [4].

The most sophisticated mathematical models of heat flow in the human torso consider the torso to consist of four concentric circular layers of different types of tissue, namely core, muscle, fat and skin (Kuznetz [6]). Models which have appeared in the literature have had at most two space dimensions and, because the effective thermal conductivity of the core is approximately the same as that of the muscle and the effective thermal conductivity of the fat is

approximately the same as that of the skin, have only two concentric layers of tissue. These layers are usually referred to as *core* and the *insulating layer*. Models which have at most two space dimensions are unable to deal with non-uniform longitudinal environmental temperatures, and those which have segments with circular cross-sections do not give realistic approximations to the geometry of the segment. This is particularly so in the case of the torso, where a cross-section is more realistically approximated by an ellipse.

The geometry of the torso and the effective thermal conductivities of its tissue types are only two of the factors governing the distribution of temperature within the segment. Other factors include the generation of heat by metabolic reaction ; convection of heat by flowing blood ; heat exchange between large arteries and veins ; heat loss due to respiration, sweating and shivering ; loss of heat at the surface of the skin due to convection, evaporation and radiation ; and environmental conditions.

Open and closed loop simulations involving these factors are dealt with in the doctoral thesis by Smith [9], whose closed loop simulations incorporate the control system developed by Stolwijk and Hardy [ll ,12,13] and validated by Konz *et al* [5].

The three dimensional form of the male human torso is such that, for a subject who is not overweight, it may be approximated extremely closely by a frustrum of an inverted elliptic cone with a long central axis. However, if a frustrum of an elliptic cone is used, making finite difference replacements to the derivatives in the differential equation and the derivative boundary conditons leads to such phenomenal difficulties that, in the opinion of the uthors, there is little to be lost in approximating the torso by an elliptic cylinder.

In the present paper, therefore, a three dimensional time dependent model of heat flow in the torso, with a constant elliptic cross-section, will be considered. The model will consist of an elliptic cylinder of core surrounded longitudinally by an annulus of muscle and surrounded totally by insulating layers of fat and skin, not of constant thickness. In any cross—section between $z = z_2$ and $z = z_3$ in Figure 1, the four tissue types will be assumed to be in the ratios 28 : 14 : 5 : 1. The torso will be considered to be that of a nude male who is not shivering or sweating and who is in an environment with windspeed that of a still room (10 cm s^{-1}). The model will be capable of dealing with a large number of different environmental temperatures surrounding the torso, even though, in practice, more than two different environmental temperatures are unlikely to be encountered. The model will also be capable of dealing with sudden changes in environmental temperature. A full stability analysis of the numerical method used to compute the temperature distribution in the torso is given. The model is tested on a number of numerical experiments.

2. THE DIFFERENTIAL EQUATIONS OF THE MODEL

Given that the torso Is to be approximated by an elliptic cylinder of length. L , the centre of whose base is at the origin (0,0,0) and whose axis lies along the positive z-axis of (x,y,z) space, the coordinates (x,y,z) of every point P within the torso and on the boundary ∂R of the region R occupied by the approximating cylinder, may be written in parametric form as

$$x = r\cos\beta \quad , \quad y = r\sin\beta \quad , \quad z = z \qquad (0)$$

where r is the distance of the point from the axis of the cylinder. Clearly $0 \leq r \leq a$, $0 \leq \beta < 2\Pi$ and $0 \leq z \leq L$, where a is the semi-major cross-sectional axis. Each point in R is thus assumed to lie on some radial line which makes an angle β with the positive semi-major axis in the plane of cross-section through the point. It is easy to show that the distance r is given by

$$r = a_p(1 - e^2\sin^2\beta)^{\frac{1}{2}},$$

where ε is the eccentricity o f the elliptic cross-section, and $a_p \leq a$ is the semi-major axis of the concentric ellipse of eccentricity e through P.

The flow of heat at the point whose parametric coordinates are given by (0), at some time $t > 0$, satisfies the heat equation

$$(\rho C)_s \frac{\partial u}{\partial t} = k_s\left\{\frac{\partial^2 u}{\partial r^2} + \frac{1}{r}\frac{\partial u}{\partial r} + \frac{1}{r^2}\frac{\partial^2 u}{\partial \beta^2} + \frac{\partial^2 u}{\partial z^2}\right\} + q_s + (m)b\ell\,(\dot{v} - u), \qquad (1)$$

where the symbols are as defined in the nomenclature. Initial and boundary conditions for (I) must be specified. The solution $u(r, \beta, z, t)$ of equation (1) gives the temperature at the point (r, β, z) in $R \cup \partial R$ at time t ; the solution v(t) gives the temperature of the blood in the

torso at time t. In equation (1) the subscript s takes the value 1,2,3,4 depending on the location of the point in the core, muscle, fat, skin respectively.

The term on the left hand side of equation (1) represents the heat stored in the torso tissues ; the first term on the right hand side represents heat transferred by conduction between tissue types, the second term represents metabolic heat generation, and the last term represents heat transferred from the tissues to the bloodstream.

It was noted in Section 1 that the effective thermal conductivities of the tissue types may be assumed to be different. There are thus discontinuities in conductivity at the interfaces between tissue types ; however, there is no discontinuity in temperature at each interface. The discontinuity in conductivity does, nevertheless, mean that equation (1) cannot be applied to points at each interface. Instead a derivative boundary condition known as *ftux equality* must be used to calculate the temperature.

Referring to Figure 1 the flux equality equations are as follows, where N denotes an outward normal to an elliptic cross-section of the torso:

(a) across AB, CD

$$- k_3 \frac{\partial u}{\partial z} = -k_4 \frac{\partial u}{\partial z}, u_3 = u_4 ; \qquad (2)$$

(b) across AD, BC

$$- k_3 \frac{\partial u}{\partial N} = -k_4 \frac{\partial u}{\partial N}, \; u_3 = u_4 ; \qquad (3)$$

(c) across EF, GH, RS, TV

$$- k_2 \frac{\partial u}{\partial z} = -k_3 \frac{\partial u}{\partial z}, \; u_2 = u_3; \qquad (4)$$

(d) across FS, GT

$$-k_1 \frac{\partial u}{\partial N} = -k_2 \frac{\partial u}{\partial N}, u_1 = u_2 ; \quad (5)$$

(e) across FG, ST

$$-k_1 \frac{\partial u}{\partial z} = -k_3 \frac{\partial u}{\partial z}, u_1 = u_3 ; \quad (6)$$

(f) across ER, HV

$$-k_2 \frac{\partial u}{\partial v} = -k_3 \frac{\partial u}{\partial N}, u_2 = u_3 , \quad (7)$$

When equations (3), (5), (7) are applied to an appropriate point P the derivatives will be written $\partial u/\partial N_p$. It is clear that, except when P is on either axis of an elliptic cross-section, $\partial u/\partial N_p$ will not intersect the axis of the cylinder. This makes the replacement of əu/əNp with finite difference approximations more difficult (see section 4). Each of the "corner points" A,B,C,D,E,F,G,H,R,S,T,V of Figure 1 is involved in two or more of equations (2) through (7). To facilitate the compilation of the linear system in Section 5, each of these points will be treated only with a flux equality equation involving əu/əz.

When applying equation (1) to points at the surface of the skin, account must be taken of the heat exchange between the skin and the environment. This exchange is governed by the derivative boundary conditions

$$-k_4 \frac{\partial u}{\partial N} = Q\{u - E(\beta(z, t)\} + s \quad (8)$$

around the curved surface of the cylinder, by

$$-k_4 \frac{\partial u}{\partial z} = Q\{u - \theta(r, \beta, t\} + s \quad (9)$$

at the top of the cylinder, and by

$$-k_4 \frac{\partial u}{\partial z} = Q\{u - \Psi(r, \beta, t)\} + s \tag{10}$$

at the bottom of the cylinder, where

$$Q = q_c + q_e + q_k + q_r \tag{11}$$

(see the nomenclature for a description of the symbols).

It will be assumed that the temperature of the blood $v = v(t)$ varies only with time and is uniform throughout the torso, as in Kuznetz [6] (models in which the temperature of the blood is not uniform are discussed in Smith [9] and Smith and Twizell [10]). The temperature of the blood is governed in the present model by a heat balance in the form of the ordinary differential equation

$$(WC)_{b\ell} \frac{dv}{dt} = \sum_{a_p}^{a} \sum_{r=0}^{a_p} \sum_{\beta=0}^{2\pi} (\dot{m}\, c)_{b\ell} (u_r^t, \beta, z - v^t). \tag{12}$$

where it is assumed that $\dot{m}$, the blood flow rate in the torso, is constant (see Kuznetz [6]), The terms $u^t_{u,\beta,z}$ and v^t are the discretized values of the continuous functions $u(r, \beta, z, t)$ and $v(t)$.

Equations (1), (10) are the differential equations of the model; the boundary conditions are given by equations (2) through (9) and initial conditions must be specified at $t = 0$. To calculate a numerical solution, the region $R \cup \partial R$ will be discretized as in the following section.

3. DISCRETIZATION IN SPACE

In the z-direction, the region R U ∂R will be discretized into M planes; let $z = Z_1, z = Z_2, z = Z_3, z = Z_4$ be the equations of the planes containing the lines AB, EFGH, RSTV, DC, respectively, in Figure 1 and define

$$\delta z_1 = \delta z_4 = \frac{z_1}{M_1^{-1}} = \frac{L - z_4}{M_1^{-1}}, \delta z_2 = \frac{z_2 - z_1}{M_2 - M_1} = \frac{z_4 - z_3}{M_4 - M_3},$$

$$\delta z_3 = \frac{z_3 - z_2}{M^3 - M_2}.$$

Clearly the z-planes are not the same distance apart. The plane $z = Z_1$ is numbered $m = M_1, z = Z_2$ is numbered $m = M_2$, $z - Z_3$ is numbered $m = M_3$ and $z = z_4$ is numbered $m = M_4$; the base of the cylinder, $z = 0$, is thus numbered $m = 1$ and the top of the cylinder, $z = L$, is numbered m. = M. The number of mesh planes in the model can hence be decided in an arbitrary fashion.

Suppose that each cross-sectional plane is discretized into K radial lines (conveniently, K is a multiple of 4) with radial line $k = 1$ along the positive semi—major axis of the cross-section and the others numbered in a counter-clockwise sense, and the number of points along each radial line including the centre point is J + 1. Because of the different thicknesses of the four tissue types, the discretization along each radial line will be taken to be different t in each tissue type. In addition, the radial discretization will be a function of the angle the radial line makes with the semi-major axis of the elliptic cross-section. Let the points at the core/muscle, muscle/fat, fat/skin interfaces be numbered $j = J_1, J_2, J_3$ respectively (for points on the axis of the cylinder $j = 0$ and for points on the curved surface $j = J$). The space steps along the K radial lines, in each tissue

type, may now be defined ; for k = 1(1)K they are

core; $h_{k1} = 4a\{1 - e^2 \sin^2 (k-1)\delta\beta\}^{\frac{1}{2}} /7J_1,$

muscle : $h_{k2} = 15a\{1 - e^2 \sin^2 (k-1)\delta\beta\}^{\frac{1}{2}} /49(J_2 - J_1),$

fat $h_{k3} = 5a\{1 - e^2 \sin^2 (k-1)\delta\beta\}^{\frac{1}{2}} /49(J_3 - J_2)$,

skin $h_{k4} = a\{1 - e^2 \sin^2 (k-1)\delta\beta\}^{\frac{1}{2}} /49(J - J_3),$

where

$$\delta\beta = 2\pi/K .$$

Defining δt to be the constant time discretization, the temperature At point j on radial line k in plane m at time t - $n\delta t$ (n = 0,1,...) will be denoted by $u^n_{j,k,m}$ and its computed value will be denoted by $u^n_{j,k,m}$ The temperature of the blood at this time will be denoted by v^n, and its computed value will be denoted by V^n It is obvious that n = 0 describes the initial conditions for all j,k,m.

The space discretization of the model requires the evaluation of (JK+1)M + 1 unknown temperatures at each time step distributed as follows :

$\{(J_1-1)K + 1KM_3-M_2-I)$: at points within the core ;

$(J_2 - J_1 - 1)K(M_3-M_2-1)$: at points within the muscle ;

$2\{(J_3-1)K + 1\}(M_2-M_1-l) + (J_3-J_2-1)K(M_3-M_2+1)$ at points within the fat ;

$(J-J_3-l)K(M_4-M_1-l) + 2\{(J-l)K+l\}(M_1-2)$ at points within the skin ;

$K(M_3-M_2+1)$: at points on the core/muscle interface ;

$2\{(J_1-i)K +1\}$: at points on the two core/fat interfaces ;

$K(M_3-M_2^+1)$: at points on the curved muscle/fat interface ;

$2\{(J_2-J_1-1)K\}$: at points on the muscle/fat interfaces in the planes $z = z_2$ and $z = z_3$ of Figure 1 ;

$K(M_4.-M_2+1)$: at points on the curved fat/skin interfaces ;

$2\{(J_3-1)K + 1\}$: at points on the fat/skin interfaces in the planes $z = z_1$ and $z = z_4$ of Figure 1 ;

KM : at points on the curved skin surface ;

$2\{(J-1)K+1\}$: at points on the upper and lower skin surfaces ;

1 : the temperature of the blood.

[Noting that $M = M_1 + M_4 - 1 = M_2 + M3 - 1$, it is easy to verify that this distribution of points does total $(JK+1)M + 1$].

The space discretization described in this section yields four simple formulas for calculating the distance of a mesh point from the central axis of the torso. Suppose the distance of the point numbered j ($j = 1,...J$) on radial line k ($k = 1,\ldots,K$) from the axis is $r_{j,k}$. , Then

$$r_{j,k} = jh_{k1} \qquad ,1 \leq j \leq J_1 \ , \qquad (13)$$

$$r_{j,k} = J_1 h_{k1} + (j-J_1)h_{k2} \qquad ,J_1 \leq j \leq J_2 \ , \qquad (14)$$

$$r_{j,k} = J_1 h_{k1} + (J_2-J_1)h_{k2} + (j-J_2)h_{k3} \qquad ,J_2 \leq j \leq J3 \ , \qquad (15)$$

$$r_{j,k} = J_1 h_{k1} + (J_2-J_1)h_{k2} + (j-J_2)h_{k3} + (j-J3)h_{k4} \qquad ,J_3 \leq j \leq J \ , \qquad (16)$$

4. FINITE DIFFERENCE REPLACEMENTS

The space derivatives in the partial differential equation (1) and its associated boundary conditions (2) through (9) may now be approximated by the following finite difference replacements as appropriate (s = 1,2,3,4 refers to a locality in the core, muscle, fat, skin respectively):

$$\frac{\partial^2 u}{\partial r^2} = (U^n_{j+1,k,m} - 2U_{j,k,m} + U^n_{j-1,k,m})/h^2_{ks} + 0(h^2_{\beta s})$$

$$\frac{\partial^2 u}{\partial \beta^2} = (U^n_{j+1,k,m} - 2U_{j,k,m} + U^n_{j,,k-1,m})/(\delta/(^2 + 0(\delta\beta)^2),$$

$$\frac{\partial^2 u}{\partial z^2} = (U^n_{j+1,k,m} - 2U_{j,k,m} + U^n_{j,,k,,m-1})/(\delta/_s)^2 + 0((\delta z_s)^2)$$

$$\frac{\partial u}{\partial r} = (U^n_{j+1,k,m} - U_{j-1,k,m})/2h_{ks} + 0(h^2_{ks}),$$

$$\frac{\partial u}{\partial r} = U^n_{j,1,k,m+1} - U_{j,k,m})\ /2\delta 2\delta_s + \ 0((\delta z_s)^2 \qquad (17)$$

$$\frac{\partial u}{\partial r} = U^n_{j,1,k,m+1} - U_{j,k,m})/\delta/_s + 0(\delta(_s) = U^n_{j,k,m} - U^n_{j,k,m-1}) + 0(\delta(_s), \qquad (18)$$

$$\frac{\partial u}{\partial r} = U^n_{j+1,k,m} - U_{j-1,k,m})/2h^*_{k4} + 0(h^{*2}_{k4}), \qquad (19)$$

$$\frac{\partial u}{\partial r} = \ U^n_{j+1,k,m} - U_{j,1,k,m})/h^*_{ks} + \ 0(h^*_{ks}) \ = \ (U^n_{j,k,m} - U^n_{j-1,k,m})/h^*_{ks} + 0(h^*_{ks}), \qquad (20)$$

where

$$h^*_{ks} = h_{ks}[(1-e^2)\{1-e^2\cos^2(k-1)^2(k-1)\delta)\delta\beta\}/\ -e^2\sin^2(k-1)\delta)\delta\beta^{\frac{1}{2}}. \qquad (21)$$

Substitution of these finite difference approximations into equation (1) and dividing by $(pC)_s$ reduces the parabolic partial differential equation to the first order ordinary differential equation

$$\frac{dU}{dt} \ = \ \left[\frac{k_s}{(\delta\delta_s)^2}\ (U^n_{j,k,m_{-1}} \ + \ U^n_{j,k,m+1}) \ + \ \frac{k_s}{r^2_{j,k}(\delta\delta\beta^2}\ (U^n_{j,k-1,m} \ + \ U^n_{j,k+1,m})\right.$$

$$+\frac{k_s}{h_{ks}}\left(\frac{1}{h_{ks}}-\frac{1}{2r_{j,k}}\right)U^n_{j-1,k,m}+\frac{k_s}{h_{ks}}\left(\frac{1}{h_{ks}}+\frac{1}{2r_{j,k}}\right)U^n_{j+1,k,m}$$

$$-\left\{\frac{2k_s}{h^2_{ks}}+\frac{2k_s}{r^2_{j,k}(\delta\beta)^2}+\frac{2}{(\delta z_s)^2}+(\dot{m}C)_{b\ell}\right\}U^n_{j,k,m}$$

$$+(\dot{m}C)_{b\ell}V^n+q_s\ ](\rho C)_s\,, \qquad (22)$$

where $r_{i,k}$ is calculated using one of formulas (13),(14),(15),(16), and s = 1,2,3,4 depending on whether $U^n_{j,k,m}$ refers to a point in the core, muscle, fat or skin.

The boundary conditions (2) through (9) are now approximated by finite differences, for k = 1(1)K, as follows:

(a) using (18) in (2) gives, for j = 1(1)J_3,

$$U^n_{j,k,M_1} = (k_4\delta z_2 U^n_{j,k,M_1-1} + K_3\delta z_1 U^n_{j,k,M_1+1})/(k_3\delta z_1 + k_4\delta z_2) + 0(\delta(_1\delta z_2) \qquad (23)$$

and

$$U^n_{j,k,M_4} = (k_3\delta z_1 U^n_{j,k,M_{4-1}} + K_4\delta z_2 U^n_{j,k,M_1+1})/(k_3\delta z_1 + k_4\delta z_2) + 0(\delta(_1\delta z_2) \qquad (24)$$

(b) using (20) in (3) gives, for m = (M_1 + 1) (1) (M_4-l),

$$U^n_{j_3,k,m} = (k_2 h^*_{k4} U^n_{J_3-1,k,m} + k_4 h^*_{k3} U^n_{j_3+1,k,m})/(k_3 h^n_{k4} + k_4 h^*_{k3}) + 0(h^*_{k3}h^*_{k4}) : \qquad (25)$$

(c) using (18) in (4) gives, for j = J_1(1)J_2,

$$U^n_{j,kM_2} = (k_3\delta z_3 U^n_{j,k,M_2-1} + k_2\delta z_2 U^n_{j,k,M_2+1})/(k_2\delta z_2 + k_3\delta z_3) + 0(\delta(_2\delta z_3) \qquad (26)$$

and

$$U^n_{j,kM_3} = (k_2\delta z_2 U^n_{j,k,M_3-1} + k_3\delta z3 U^n_{j,k,M_3+1})/(k_2\delta z_2 + k_3\delta z_3) + 0(\delta(_2\delta z_3) \qquad (27)$$

(d) using (20) in (5) gives, for m = $(M_2+1)(1)(M_3-1)$,

$$U^n_{j_1,k,m} = (k_1 h^*_{k2} U^n_{j_1-1,k,m} + k_2 h^*_{k1} U^n_{j1+1,k,m})/(k_1 h^*_{k2} + k_2 h^*_{k1}) + 0(h^*_{k1} h^*_{k2}); \quad (28)$$

(e) using (18) in (6) gives, for j = $1(1)J_1$,

$$U^n_{j,k,M_2} = (k_3 \delta z_3 U^n_{j,k,M_2-1} + k_1 \delta z_2 U^n_{j,k,M2+1})/(k_1 \delta z_2 + k_3 \delta z_3) + 0(\delta(_2 \delta z_3) \quad (29)$$

and

$$U^n_{j,k,M_3} = (k_1 \delta z_2 U^n_{j,k,M_3-1} + k_3 \delta z_3 U^n_{j,k,M_3+1})/(k_1 \delta z_2 + k_3 \delta z_3) + 0(\delta(_2 \delta z_3) \quad (30)$$

(f) using (20) in (7) gives, for m = $(M_2+1)(1)(M_3-1)$,

$$U^n_{J_2,k,m} = (k_2 h^*_{k3} U_{J2-1,k,m} + k_3 h^*_{k2} U_{J2+1,k,m})/(k_2 h^*_{k3} + h^*_{k2}) + 0(h^*_{k2} h^*_{k3}); \quad (31)$$

(g) using (19) in (8) gives, for m = 2(1)(M-1),

$$U^n_{J+1,k,m} = U^n_{J-1,k,m} - 2k_4^{-1} h^*_{k4} Q U^n_{J,k,m} + 2k_4^{-1} h^*_{k4} Q E^n_{k,m} - 2k_4^{-1} h^*_{k4} s + 0(h^{*3}_{k4}) \quad (32)$$

where $\theta^n_{k,m}$ is the value of the environmental temperature adjacent to the point where radial line k (k = 1,...,K) at z-level m (m = 1,...,M) meets the curved skin surface, at time t = nδt ;

(h) using (17) in (9) gives, for j

$$(U^n_{j,k,M+1} = U^n_{j,k,M-1} - 2k_4^{-1} \delta z_1 Q U^n_{j,k,M} + 2k_4^{-1} \delta z_1 Q \theta^n_{j,k} - 2k_4^{-1} \delta z_1 s + 0(\delta(^3_1) \quad (33)$$

where $\theta^n_{k,m}$ is the value of the environmental temperature above the point numbered j on radial line k on the top surface of the torso, at time t = nδt ;

(i) using (17) in (10) gives, for j = 1(1)J,

$$U^n_{j,k,0} = U^n_{j,k,2} + 2k_4^{-1} \delta z_1 Q U^n_{j,k,1} - 2k_4^{-1} \delta z_1 Q \psi^n_{j,k} + 2k_4^{-1} \delta z_1 S + 0(\delta(^3_1) \quad (34)$$

where $\psi^{n}_{j,k}$ is the value of the environmental temperature below the point numbered j on radial line k on the bottom surface of the torso, at time $t = n\delta t$.

The temperatures $U^{n}_{j+k,l,m}$, $U^{n}_{j,k,m+1}$, $U^{n}_{j,k,o}$ in equations (32),(33),(34) are, of course, abstract in that they refer to points outside the skin surface. They will however be required when equation (22) is applied to points on the skin surface.

In applying equation (22) to points on radial line $k = 1$, it is clear that points on radial line K will be used for radial line 0 (zero); similarly, points on radial line 1 will be used for radial line $K + 1$ when equation (22) is applied to points on radial line K.

Equation (22) cannot be applied to points on the central axis of the torso, that is for $j = 0$, These axis points will, however, be required when equation (22) is applied to those points where $j = 1$ (any k, any m). The temperature at time $t = n\delta t$ at the axis points will be estimated using the formula

$$U^{n}_{0,k,m} = \left(\sum_{k=1}^{k} U^{n}_{1,k,m} \right) \Big/ k \qquad (35)$$

as in Smith [8 ;p.40].

It is not necessary to make finite difference replacements in equation (12). This equation will however be used in the more convenient form

$$\frac{dV^{n}}{dt} = \left(\frac{\dot{m}}{w} \right)_{b\ell} \sum_{m=1}^{M} \sum_{k=1}^{K} \sum_{j=1}^{j} U^{n}_{j,k,m} - \left(\frac{\dot{m}}{w} \right)_{b\ell} JKMV^{n} \qquad (36)$$

when compiling the system of linear ordinary differential equations governing the distribution of temperature in the torso.

5, IMPLEMENTATION

Applying equation (22) to every point of $R\ U$ əR which is not on the central axis or on one of the tissue interfaces and equation (36) to the blood, leads to a system of first order ordinary differential equations of the form

$$\frac{d\underline{U}}{dt} = A\underline{U} + \underline{b}. \tag{37}$$

The order of this system is equal to the number of mesh points not on the central axis or on the interfaces, plus one (the temperature of the blood). The order η is thus given by

$$\eta = (J - J_3 + 1)KM_1 + (J_3K + K + 1)M_2 + (J_3K - 3K + 1)M_3 + (J - J_3 -)JM_4 + (K - 1)M - (J + 2J_2 + 2J_3 - 4)K. \tag{38}$$

The column vector $\underline{U}$ of order η is the vector whose first η - 1 elements are the computed values of tissue temperature and whose last element is the computed value of the temperature of the blood. The square matrix A is sparse, of order η and contains the coefficients of the computed values of u and v ; these coefficients are obtained from equations (22) through (36). The column vector $\underline{b}$ is also of order η whose elements contain the terras q_m (m = 3,2,3,4) and the environmental temperatures adjacent to the skin.

The ordering of the elements of the vector $\underline{U}$ is obtained by listing the points on each radial line in each z-plane to which equation (22) may be applied, together with the temperature of the blood. Visual examination of Figure 1 shows that the M z-planes can be conveniently divided into nine classes in the ordering process.. These classes together with the temperature of the blood, are as follows:

(i) planes 1,..., M_1-1;

(ii) plane M_1 ;

(iii) planes M_1+l,...,M_2-1 ;

(iv) plane M_2 ;

(v) planes M_2+1,...,M_3-1 ;

(vi) plane M_3 ;

(vii) planes M_3 +1,... ,M_4-1 ;

(viii) plane M_4 ;

(ix) planes M_4 + 1,...,M ;

(x) temperature of the blood.

In each z-plane, the mesh points to which equation (22) may be applied are ordere d outwards from the central axis along each radial line in turn. A comprehensive listing of the elements of $\underline{U}$ is given in Appendix I, where the ten classes listed above are separated by broken lines, planes are separated by colons and radial lines by semi-colons.

The matrix A has one row corresponding to each element of the vector $\underline{U}^n$ The non-zero elements of A depend on the coefficients of the elements of $\underline{U}^n$ in equation (22), the boundary conditions (23) through (34), equation (35), and blood heat balance equation (35).

The elements of the vector $\underline{b}^n$ depend on the heat source terms s = 1,2,3,4, in equation (22), and the physiological-terms and $q_s/(\rho c)_s$, environmental temperatures arising in equations (32) , (33) , (34) ,

The rows of the matrix A and the elements of the vector $\underline{b}^n$ are clearly combined in the same order as the elements of the vector $\underline{U}^n$.

6. ANALYSIS OF COMPUTED SOLUTIONS

It is easy to show that the formal solution of the system of ordinary differential equations (22) is given by

$$\underline{U}(t) = (\exp\ tA)(\ \underline{g} + A^{-1}\underline{b}) - A^{-1}\underline{b}, \tag{39}$$

where $\underline{g}$ is the vector of order η giving the initial values of u and v. The elements of $\underline{g}$ are compiled in the same order as $\underline{U}$, and in (39) the vector $\underline{b}$ is evaluated at time t.

Equation (39) satisfies the recurrence relation

$$\underline{U}(t + \delta t) = (\exp \delta e\ A)\{\underline{U}(t) + A^{-1}\ \underline{b}\} - A^{-1}\underline{b} \tag{40}$$

which may be used to determine a numerical solution of equation (1) by making a suitable approximation to the matrix function (exp δt A).

The accuracy in time and the numerical stability of any computed solution derived from (40) will clearly depend on the chosen approximation to exp (δt A) and, ultimately, stability will depend on the eigenvalues of the matrix A. It is obvious from equations (22) through (36) that the matrix A has very complicated elements and its eigenvalues are thus difficult to determine. However, it can be shown using Brauer's theorem (see, for example, Smith [8 ;p.88]), that the eigenvalues of A are non-positive. This exercise is carried out in detail, by the authors, for a two space dimension model of heat flow in the torso, using a circular cross section, in [16]. Each eigenvalue λ of the present model is seen to satisfy an inequality of the form

$$-\frac{1}{(h_{ks}\delta\beta\ \delta z_r)^2}\ p_i \leq \lambda \leq 0 \tag{41}$$

or

$$-\frac{1}{(h_{ks}\delta\beta\ \delta z_r)^2}\ p_i \ \le\ \lambda\ \le\ -p_i^*, \tag{42}$$

where r,s = 1,2,3,4 and k = I(1)K, In the model proposed in the present paper there can be at most 109 different P_i. The P_i, p_i^* depend only on the physiological constants and are therefore positive ; the eigenvalues of the matrix A are thus non-positive.

Choosing the (0,1) Padé approximant to exp(δt A) in (40) gives the first order formula

$$\underline{U}(t\ +\ \delta tA)\ \underline{U}(t)\ +\ \delta t\ \underline{b}^n\ +\ 0((\delta t))^2)\ , \tag{43}$$

where I is the identity matrix of order η . This leads to an explicit finite difference scheme which, like any other explicit scheme, is easy to implement. However, the amplification factor is $2/\max_i\{p_i\}$, showing that the scheme has a severe stability restriction.

Choosing the (1,0) Padé approximant to exp(δt A) in (40) gives the first order formula

$$(I\ -\ \delta tA)\ \underline{U}\ (t\ +\ \delta t)\ -\ \delta t\underline{b}^{n+1}\ =\ \underline{U}(t)\ +\ 0((\delta t)^2) \tag{44}$$

Defining $\underline{Z}^n$ to be the difference between the theoretical and computed solutions of the implicit finite scheme resulting from (44) at time t = nδt, it is easy to see that

$$\underline{Z}^{n+1}\ =\ (I\ -\ \delta t\ A)^{-1}\ \underline{Z}^n$$

and, since the eigenvalues of A are non-positive, it follows that $\left|\underline{Z}^{n+1}\right| \le \left|\underline{Z}^n\right|$ The finite difference scheme resulting from (44) is thus unconditionally stable and large time steps may be taken. The scheme does, however, require the solution of a linear system of order η at every time step.

Second order accuracy may be attained by choosing the (1,1) Padé

approximant to the exponential matrix function in (40). This approximation leads to a Crank-Nicolson type finite difference scheme given in vector form by

$$(I - \frac{1}{2}\delta tA)\underline{U}(t + \delta t) - \frac{1}{2}\delta t\underline{b}^{n+1} = (I + \frac{1}{2}\delta tA)\underline{U}(t) + \frac{1}{2}\delta t\underline{b}^{n} + 0(\delta t)^3). \qquad (45)$$

The error $\underline{Z}^n$ satisfies the relation

$$\underline{z}^{n+1} = (I - \frac{1}{2}\delta t\ A)^{-1}(I + \frac{1}{2}\delta t\ A)\ \underline{Z}^n$$

from which it is clear that the finite difference scheme is unconditionally stable, the amplification factor tending asymptotically to -1. This scheme also requires the solution of a linear system of order η.

Like the explicit scheme (43), the Crank-Nicolson type scheme (45) does not cope satisfactorily with discontinuities between initial conditions and boundary conditions. Such discontinuities arise with instantaneous changes in environmental temperature and can be encountered in space travel, industrial environments and naturally extreme environments. When such discontinuities do arise, the explicit scheme and the Crank-Nicolson type scheme give poor computed results near the skin surface. The backward difference scheme based on the (1,0) Padé approximant does not have this drawback and gives acceptable results near the skin surface. Lawson and Morris [7] give an example of the behaviour of methods based on the (1,0) and (1,1) Padé approximants near the boundaries in a diffusion problem with discontinuities between initial conditions and boundary conditions.

In view of the likelihood of discontinuities between initial conditions and boundary conditions in the important situations where numerical modelling of heat flow in the human torso is most valuable, only the

method based on the (1,0) Padé approximant, given by equation (44), will be discussed further. It is this method which will be used in the numerical experiments discussed in Section 9.

7. EXTRAPOLATION OF THE (.1,0) METHOD

It was seen in Section 6 that the backward difference method (44) based on the (.1,0) Padé' approximant is only first order accurate in time (error = $0(\delta t)^2)$), one order fewer than the Crank-Nicolson type method (45). The (1,0) method will now be extrapolated to give the same order accuracy as the Crank-Nicolson type method (45), the extrapolated form of (44) dealing satisfactorily with any discontinuities between initial conditions and boundary conditions.

Following Lawson and Morris [7], the finite difference scheme yielded by equation (44) may be written over two single time steps of δt as

$$\underline{U}^{(1)}(t + 2\delta t) = (I - \delta tA)^{-1}(I - \delta tA)^{-1}\{\underline{U}(t) + A^{-1}\underline{b}^n$$

$$= (I + 2\delta tA + 3(\delta t)^2 A^2\{\underline{U}(t) + A^{-1}\underline{b}^n\} - A^{-1}\underline{b}^n + 0((\delta t)^3) \quad (46)$$

and over a double time step $2\delta t$ as

$$\underline{U}^{(2)}(t + 2\delta t) = (I - 2\delta tA)^{-1}(I - \delta tA)^{-1}\{\underline{U}(t) + A^{-1}\underline{b}^n$$

$$= (I + 2\delta tA + 4(\delta t)^2 A^2\{\underline{U}(t) + A^{-1}\underline{b}^n\} - A^{-1}\underline{b}^n + 0((\delta t)^3) \quad (47)$$

Comparing (46) and (47) with the Maclaurin expansion

$$\underline{U}^{(M)}(t + 2\delta t) = \exp(2\ \delta xp(\ \{\underline{U}(t) + A^{-1}\underline{b}^n\} - A^{-1}\underline{b}^n$$

$$= (I + 2\delta tA + 2(\delta t)^2 A^2\{\underline{U}(t) + A^{-1}\underline{b}^n\} - A^{-1}\underline{b}^n + 0((\delta t)^3). \quad (48)$$

It is easy to see that neither is second order accurate but that $\underline{u}^{(E)} = \underline{U}^{(E)}(t + 2\delta t)$ defined by

$$\underline{U}^{(E)} = 2\underline{U}^{(1)} - \underline{U}^{(2)} = \underline{U}^{(M)} + 0((\delta t)^3) \quad (49)$$

does achieve second order accuracy in time. Accuracy higher than second order may be achieved using the techniques developed in Gourlay and Morris [2] or Twizell and Khaliq [15].

The implementation of the extrapolation algorithm (49) is described in

detail in Smith [9] and is outlined here for time $t = n\delta t$ $(n= 0,1,2,...)$; the initial distribution $\underline{U}$ is discussed in Section 8:

(1) compute $\underline{b}^n$, $2\delta t\ \underline{b}^n$, $(\delta t)^2 A^2 \underline{b}^n$, $(I - \delta t\ A)$, $(I - 2\delta t\ A)$;

(2) compute $\underline{U}^n + 2\delta t\ \underline{b}^n - (\delta t)^2 A\ \underline{b}^n$ and use a direct method of solution (Gaussian elimination with pivoting) to solve the equation $(I - \delta t\ A)\underline{U}^* = \underline{U}^n + 2\delta 1\ \underline{b}^n - (\delta t)^2 A\ \underline{b}^n$ for the intermediate vector $\underline{U}^*$;

(3) solve $(I - \delta t\ A)\ \underline{U}^{(1)} = \underline{U}^*$ for $\underline{U}^{(1)}$ using a direct method ;

(4) compute $\underline{U}^n + 2\delta t\ \underline{b}^n$ and use a direct method of solution to solve $(I - 2\delta t\ A)\ \underline{U}^{(2)} = \underline{U}^n + 2\delta t\ \underline{b}^n$ for $\underline{U}^{(2)}$;

(5) use $\underline{U}^{(E)} = 2\underline{U}^{(1)} - \underline{U}^{(2)}$ to compute $\underline{U}^{n+2} = \underline{U}(t + 2\delta t)$;

(6) let $\underline{U}^n := \underline{U}^{n+2}$, compute new $\underline{b}^n$, and return to step (2).

8. INITIAL CONDITIONS

To begin the computation, the initial vector $\underline{U}^0$ is required. This vector will depend on the initial temperature distributions $E^0_{k,m}$ $\theta^0_{j,k,}$ $\psi^0_{j,k}$ ($m = 1, \ldots, M$; $j = 1, \ldots, J$; $k = 1 \ldots\ldots, K$) used in equations (32),(33),(34).

It is assumed that the temperature distribution within the torso and on the skin surface is in a steady state initially. The mathematical method then determines the vector $\underline{U}$ after an instantaneous change in the environmental temperature.

The initial temperature distribution, including the initial temperature of the blood, is found by solving the initial equation

$$A\,\underline{U}^0 + \underline{b}^0 = \underline{0} \qquad (50)$$

where $\underline{0}$ is the null vector of order η.A direct method such as Gaussian elimination may be used to solve equation (50) for $\underline{U}^0$.

9, NUMERICAL RESULTS

The numerical experiments consider a nude male subject who is in equilibrium with the environment and who is not shivering or sweating. The physiological constants for the subject (described in the nomenclature) have the numerical values given in Table 1. The wind-speed is taken to be 0,1 m s^{-1}.

The length of the torso is taken to be L = 40 cm, the semimajor axis of a cross section is taken to be 16 cm and the semiminor axis to be 12 cm ; the eccentricity is thus $e = \frac{1}{4}\sqrt{7}$. In any cross-sectional plane z, such that $z_2 \leq z \leq Z_3$ in Figure 1, the thicknesses of the core, muscle, fat, skin are in the ratios 28 : 14 : 5 : 1 along any radial line. The maximum thicknesses of the four tissue types in any of these planes are therefore $\frac{28}{3}$ cm, $\frac{14}{3}$ cm, $\frac{5}{3}$ cm, $\frac{1}{3}$ cm, respectively. Taking $J_1 = 6$, $J_2 = 10$, $J_3 = 14$, $J = 17$ gives $h_{11} = \frac{14}{9}$ cm, $h_{12} = \frac{7}{6}$ cm $h_{13} = \frac{5}{12}$ cm, $h_{14} = \frac{1}{9}$ cm. It is assumed that the thicknesses of the fat and skin at the top and bottom of the model torso are $\frac{5}{3}$ cm and $\frac{1}{3}$ cm, respectively. Then, taking $M_1 = 4$, $M_2 = 8$, $M_3 = 13$, $M_4 = 17$, $M = 20$ gives $\delta_{z1} = \delta_{z4} = \frac{1}{9}$ cm, $\delta_{z2} = \frac{5}{12}$ cm, and $\delta_{Z3} = \frac{36}{5}$ cm. The number of radial lines in each cross section is taken to be K = 12, so that $\delta\beta = \pi/6$.

The space discretization of the model for the numerical experiments, as described in the previous paragraph, involves 3265 unknown temperatures, including the temperature of the blood, to be determined using equation (44), together with 836 temperatures on the tissue interfaces and the central axis, to be determined using equations (23) through (35). In practice, this large number of unknowns can invariably be reduced by fully exploiting symmetry.

The temperature of the environment at time $t = 0$ is assumed for both experiments to be uniformly distributed around the torso and to have the value 25^0 C. The temperature distribution in the torso at time $t = 0$ is found by solving a linear system of type (50). The initial distribution along radial line $k = 4$ (from the central axis along the positive semi-minor axis to the front of the torso) in cross-sectional plane $m = 11$, is depicted in Figure 2. It was found that the temperature of the skin in this steady state was uniformly distributed with the approximate value 33.3^0 C : the maximum deviation from this value was 0.01^0 C, this figure being due to round off in solving (50). It was also found that the temperature of the blood was 37.0^0 and that the temperature of most of the core and muscle was just below this value in the range 36.7^0 C $\leq u \leq 36,9^0$ 0C ; the substantial drop in temperature did not occur until the muscle/fat interface had been passed ($j = 11$).

Using this steady state temperature distribution as initial conditions, the model was tested, in the first experiment, on one of the experiments of Hall and Klemm [3]. Instantaneously, the subject first faces a wall at 93^0 C with his back to a wall at -6.7^0 C ;after 30 minutes the subject reverses himself (the model is thus subjected to two sets of discontinuity).Retaining the space discretization used to determine the initial conditions,the distribution of environmental temperatures for this first experiment is constant and is as follows for all n =1,2,.,.;

$$\theta^n_{j,k} = \psi^n_{j,k} = 93^0\text{c for} k = 1(1)7, = j = 0(1)17 ;$$

$$\theta^n_{j,k} = \psi^n_{j,k} = -6.7^0\text{C for } k = 8(1)12 = j = 1(1)17 ;$$

$$E^n_{k,m} = 93^0\text{C for } m = 2(1)19, \quad k = 1(1)7;$$

$$E^n_{k,m} = -6.7^0\text{C for } m = 2(1)19, \quad k = 8(1)12;$$

A time step $\delta t = ½$ minute was used and symmetry was fully exploited in computing the temperature distribution as time increased, allowing storage requirements to fall to about 30% of the maximum requirement.

Numerical results were obtained using the backward difference scheme (44) to calculate the temperature at mesh points not on the tissue interfaces and the temperature of the blood. Equations (23) through (35) were then used to compute the temperature at mesh points on the tissue interfaces. The computed temperatures at the skin surface on radial line 10 (the middle of the back) and at the skin surface on radial line 4 (the front of the chest) in cross-sectional plane m =11 are depicted in Figure 3.

Comparing the results yielded by the model with the computed results of Kuznetz [6] and the laboratory results of Hall and Klemm [3], which are also depicted in Figure 3, it is seen that the computed results of the present model are, in part, closer the the laboratory results of Hall and Klemm [3] than the computed results of Kuznetz [6]. For some of the time interval the two curves in Figure 3 representing the computed results are superimposed.

The computed results obtained so far in this first experiment play a significant part in the validation of the numerical model described in this paper.

The computed results were then extrapolated using the strategy outlined in Section 7. The extrapolation of the computed temperatures at the extremities of the minor axis of cross-sectional plane m = 11 , are also depicted in Figure 3. The curve representing the extrapolated results shows a marked improvement, especially in the time interval $0 < t < 30$ minutes where the numerical results were reasonably close

to the laboratory results of Hall and Klemm [3]. The extrapolated temperature of the blood, which was very close to that of the centre of plane m = 11, together with the rectal temperature measured by Hall and Klemm, are also shown in Figure 3. There is close agreement here, too, between the computed results of the new model and the laboratory results.

It is clear that the numerical model described in this paper deals successfully with discontinuities between initial conditions and boundary conditions. The model also simulates successfully the ability of the torso to maintain a comfortable temperature in disparate environments. It was noted that the mean temperature of the skin was nearly normal throughout the experiment and that maximum temperature of the skin surface did not exceed the safe pain threshold touch limit of 45^0 C (Kuznetz [6]). As with the experimental results of Hall and Klemm [3], and the model results of Kuznetz [6], the numerical results for this first experiment seem to be reaching a steady state at t = 80 minutes. The steady state temperature distribution in cross-sectional plane m= 11 from the posterior skin surface along radial line 10, across the central axis, then along radial line 4 to the anterior skin surface, is depicted in Figure 4,

The second numerical experiment is designed to utilize the model's ability to deal with three-dimensional diffusion in the torso. The top half of the torso is subjected instantaneously to the two extreme environmental temperatures of the first experiment, whilst the environmental temperature surrounding the bottom half of the torso is maintained at the initial temperature of 25^0 C. The distribution of environmental temperatures for the second experiment for all n = 1,2,... is thus:

$$\psi^{n}_{j,k} = 25^{0}\,c \qquad \text{for} \quad k = 1(1)12\,, \quad j = 0(1)17 \quad ;$$

$$E^{n}_{k,m} = 25^{0}\,c \qquad \text{for} \quad m = 2(3)10\,, \quad k = 1(1)12 \quad ;$$

$$E^{n}_{k,m} = 93^{0}\,c \qquad \text{for} \quad m = 11(1)19\,, \quad k = 1(1)7 \quad ;$$

$$E^{n}_{k,m} = -6.7^{0}\,c \qquad \text{for} \quad m = 31(1)19\,, \quad k = 8(1)12 \quad ;$$

$$\theta^{n}_{j,k} = 93^{0}\,c \qquad \text{for} \quad k = 1(1)7 \quad , \quad j = 0(1)17 \quad ;$$

$$\theta^{n}_{j,k,} = -6.7^{0}\,c \qquad \text{for} \quad k = 8(1)12 \quad , \quad j = 1(1)17 \quad .$$

A time step $\delta t = \frac{1}{3}$ minute was used and numerical results were obtained using the backward difference scheme (44) and the extrapolation procedure described in Section 7. The model did not reverse himself in the second experiment.

Computed results were obtained using the method based on the (1,0) Padé approximant given by (44) to determine the temperatures within the tissues, and equations (23) through (35) to determine the temperatures at points on the tissue interfaces. The computed results were extrapolated using the strategy described in Section 7.

The extrapolated temperatures at the skin surface (j = 17) on radial line 4 (the front of the chest) in cross-sectional plane m= 11, at the skin surface on radial line 4 in cross-sectional plane m = 10, and at the skin surface on radial line 10 in cross-sectional plane m = 11 are depicted in Figure 5, It was noted that the temperatures at the points on the skin surface on radial lines 4 and 10 in cross-sectional plane m = 1 I appeared to be converging to the same values as those attained in the first numerical experiment. It was further found that convergence took place more quickly than in the first experiment, due, it is suspected, to the intermediate environmental temperature of 25^{0} C

between the two extreme environmental temperatures of -6.7 ^{0} C and 93^{0} C.

There are no other references to the second experiment in the literature. The success of the model in closely duplicating the laboratory results in the first experiment, indicates that the results obtained in the second experiment are reliable and that the model has been validated for use with environmental temperatures which vary with all three space dimensions.

10. SUMMARY

A three dimensional, time dependent model of heat flow in the human torso has been considered in the present paper. The torso has been approximated by an elliptic cylinder of core surrounded longitudinally by an annulus of muscle and surrounded totally by insulating layers of fat and skin.

The space derivatives in the parabolic partial differential equation governing the flow of heat in the torso, and in the derivative boundary conditions at the skin surface and at the interfaces of tissue types, were approximated by finite difference replacements. This resulted in a system of first order ordinary differential equations the solution of which involved the exponential matrix function.

The exponential matrix function was replaced by the (1,0) Padé approximant, giving an implicit method for computing a numerical solution. The implicit method was analysed for stability and an extrapolation procedure developed for improving the accuracy in time.

An experiment carried out in a US Air Force laboratory and duplicated in a NASA mathematical model, was repeated. The numerical results obtained were seen to validate the model which was further tested on a second, related numerical experiment. The model was seen to cope satisfactorily with discontinuities between initial conditions and boundary conditions which arise when the environmental temperature changes instantaneously.

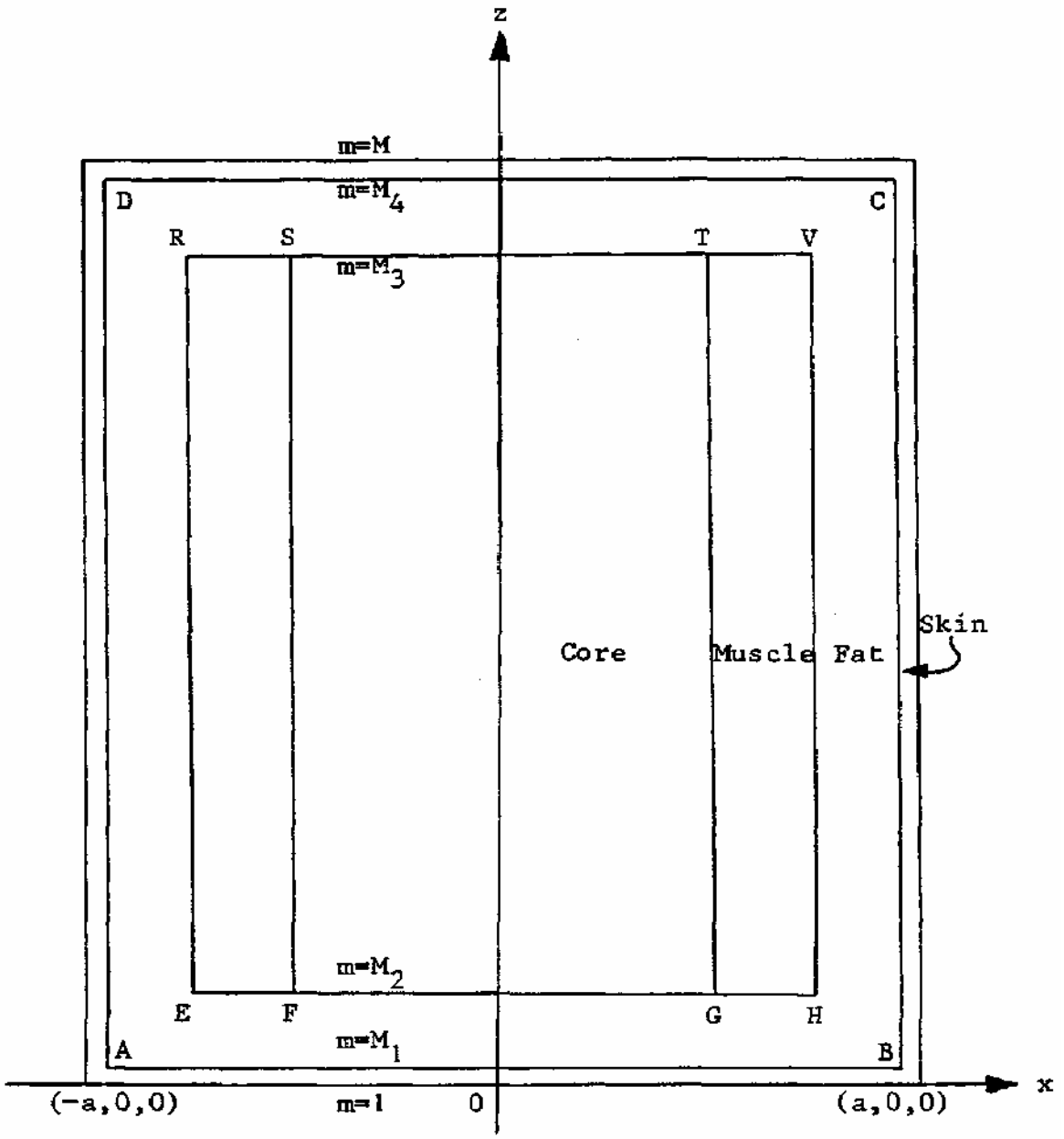

Figure 1 : Cross-section in the x-z plane showing the four tissue types.

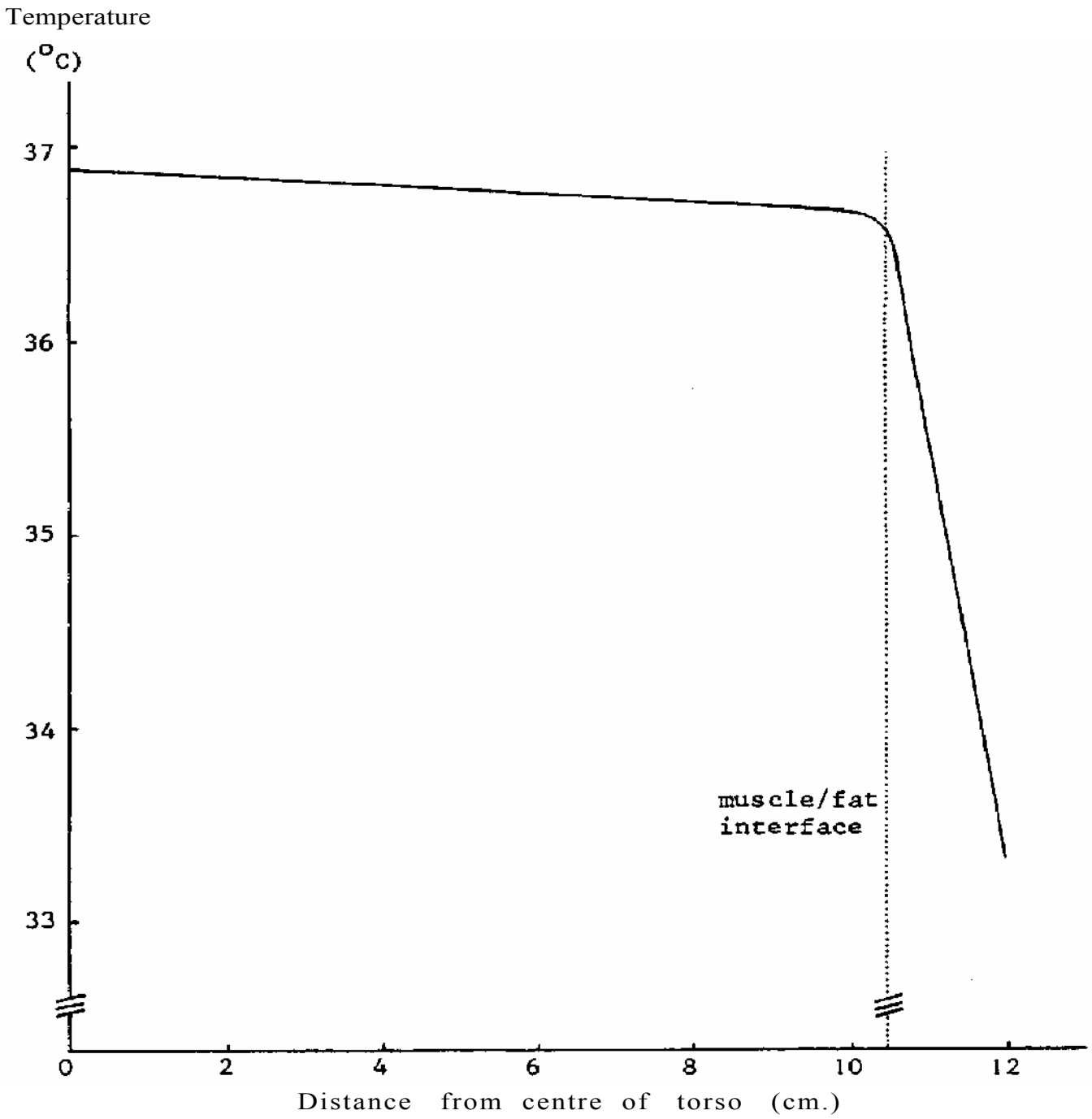

Figure 2 : Initial temperature distribution from the central axis to the skin surface on the chest.

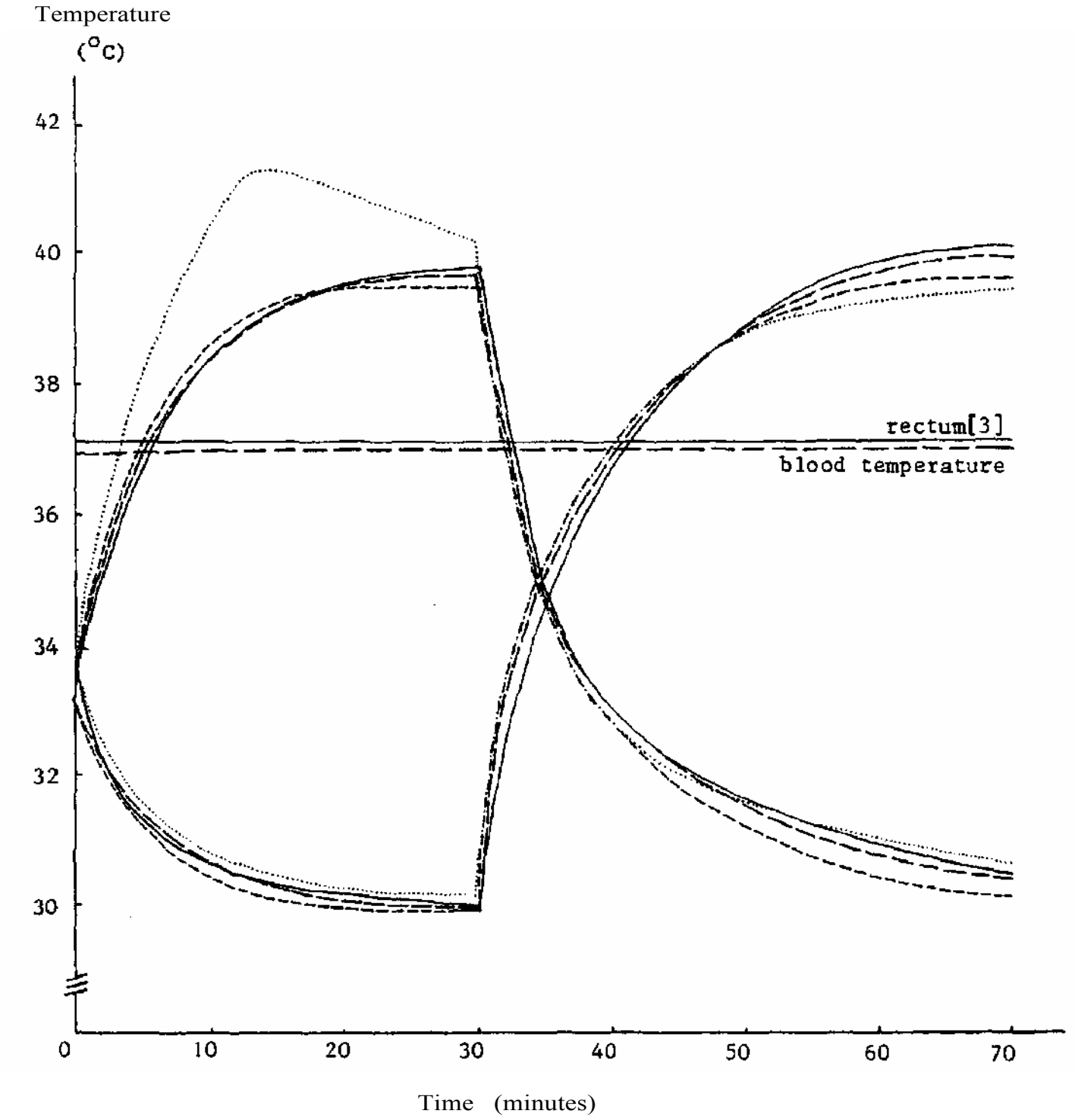

Figure 3 : Results of first experiment : _____ .Laboratory results of Hall and Klemm[3]; ..... Kuznetz[6]; _____ Kuznetz[6] and Twizell and Smith;---------- Twizell and Smith; _____ Extrapolated form of Twizell and Smith.

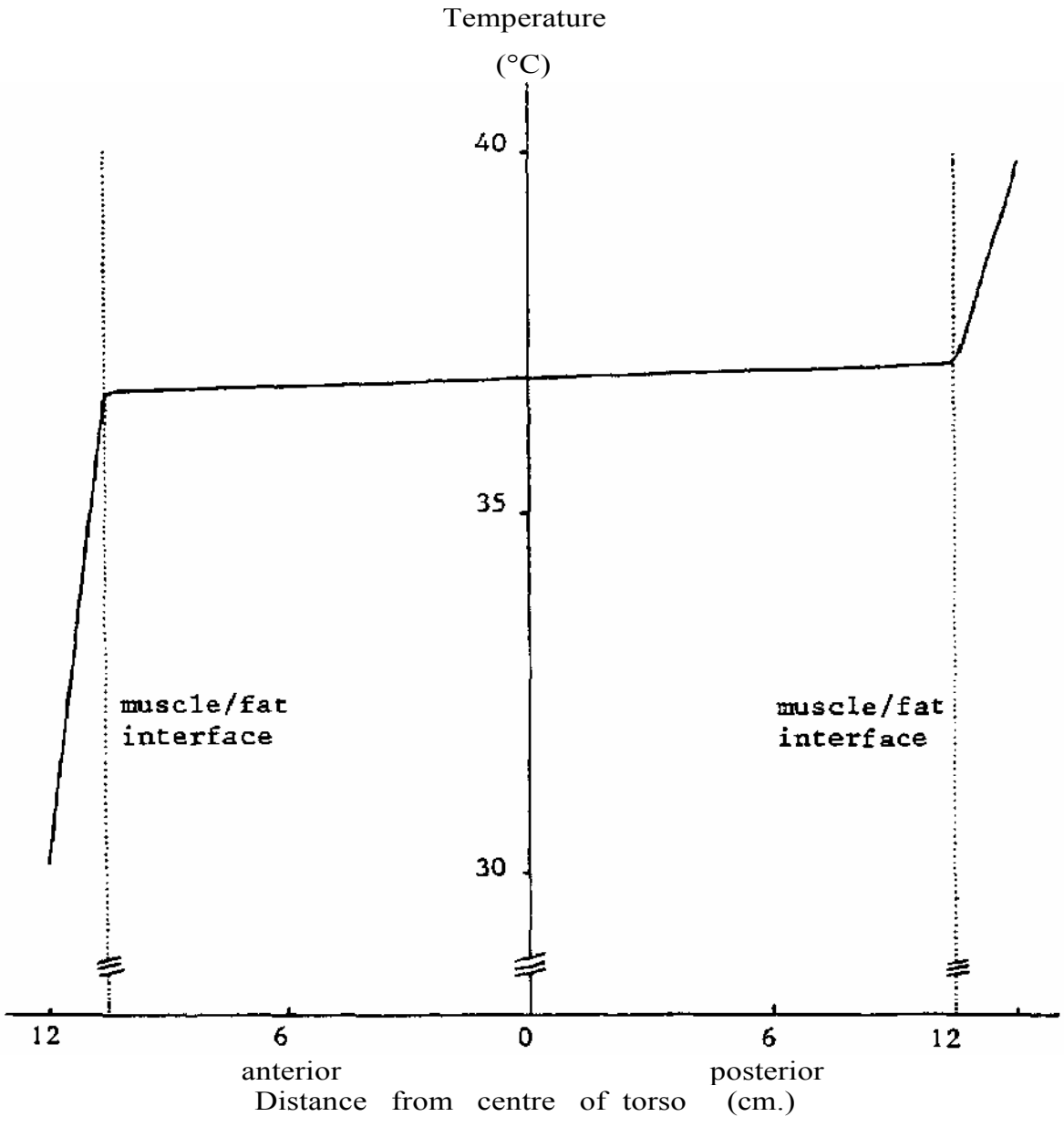

Figure 4 : Steady state temperature distribution in the y-z plane at the end of the first experiment.

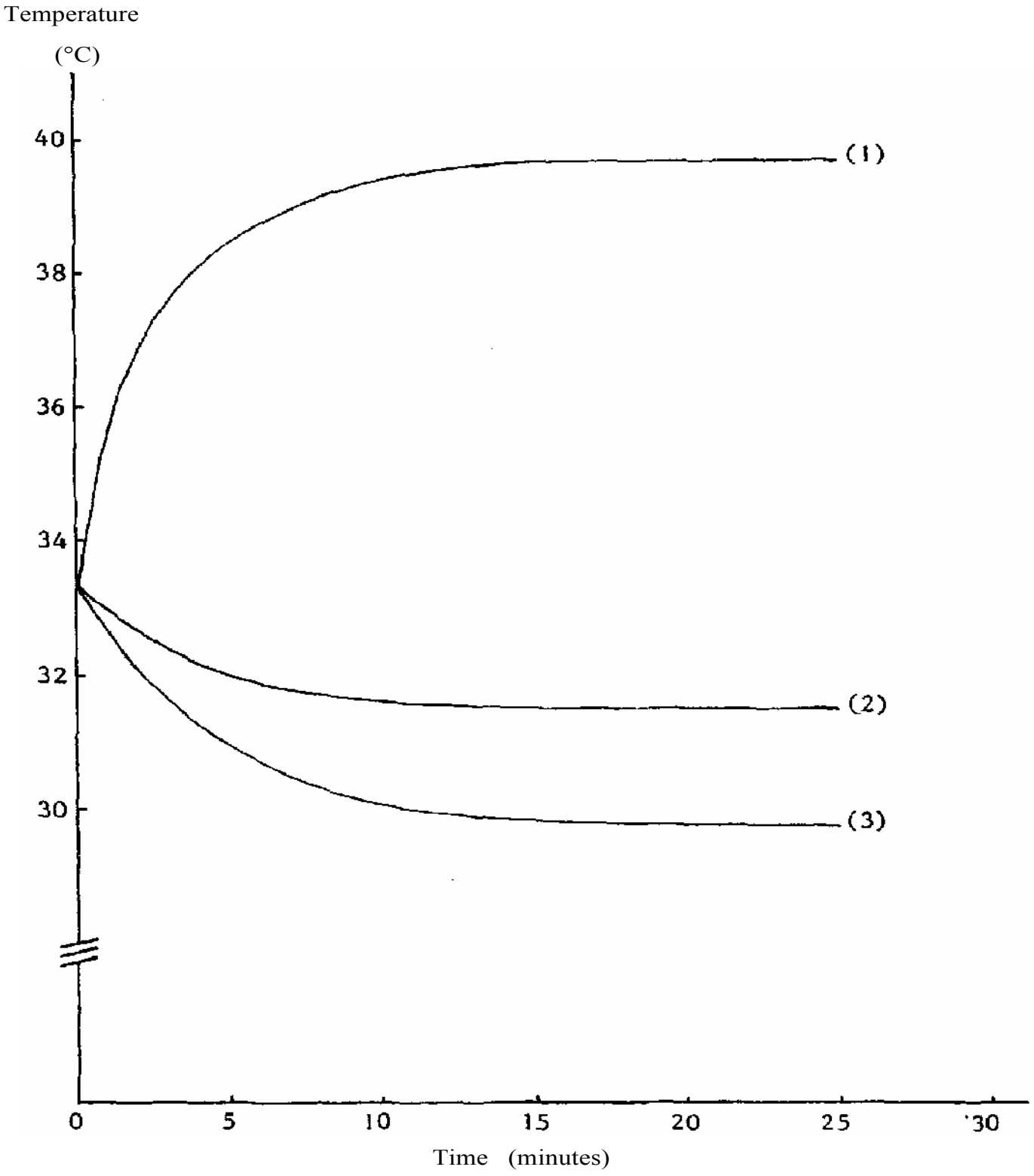

Figure 5 : Temperature at the skin surface (j = 17) for the second experiment:
(1) k=4,m=11; (2) k=4,m=10; (3) k=10,m=11.

Table 1 : Numerical values of physiological constants

Constant	Value
$(\rho c)_1$, $(\rho c)_2$	3344000 J m^{-3} °c^{-1}
$(\rho c)_3$, $(\rho c)_4$	2926000 J m^{-3} °c^{-1}
k_1 , k_2	0.418 W m^{-1} °C^{-1}
k_3 , k_4	0.209 W m^{-1} °C^{-1}
q_1 , q_2	1339 W m^{-3}
q_3 , q_4	423 W m^{-3}
$(\dot{m} C)_{b\ell}$	0.232 W °C^{-1}
Q	7.0826 W m^{-2} °C^{-1}
s	4.9909 W m^{-2}
$(\dot{m}/_w)_{b\ell}$	0.016 S^{-1}

REFERENCES

1. Fan, L.-T. , F.-T. Hsu, . and C.-L. Hwang, "A review of mathematical models of the human thermal system", *IEEE Transactions on Biomedicail Engineering* BME - 18 (3) : 218 - 234, 1971.

2. Gourlay ,A.R, and J. LI. Morris, "The extrapolation of first order methods for parabolic partial differential equations II", *SIAMJ. Numer. Anal.* 17(5) : 641 - 655, 1980.

3. Hall, J.F. Jr., and F.K . Klemm, "Thermal comfort in disparate thermal environments" ,J. *Appl. Physiol.*, 27 : 601 - 606, 1969.

4. Hwang, C.—L. , and S . A. Konz, "Engineering models in the human thermoregulatory system — a review", *IEEE Transactions on Biomedical Engineering* BME - 24(4) : 309 - 325, 1977.

5. Konz, S., C. Hwang, B. Dhiman, J. Duncan, and A. Masud, "An experimental validation of mathematical simulation of human thermoregulation", *Comput. Biol. Med, 7 :* 71 - 82, 1977.

6. Kuznetz, L.H. , "A two-dimensional transient mathematical model of human thermoregulation", Am. J. *Physiol.* 237 (5) : R266 - R277, 1979,

7. Lawson, J.D. , and J,LI. Morris, "The extrapolation of first order methods for parabolic partial differential equations II", *SIAM J. Numer. Anal.* 15(6) : 1212 - 1224, 1978.

8. Smith, G.D., *Numerical Solution of Partial Differential Equations ; Finite Difference Methods* (second edition), Oxford, Oxford University Press , 1978.

9. Smith, P. , *Numerical Modelling of Human Thermoregulation.* Doctoral thesis, C.N. A. A. , 1981.

10. Smith, P., and E.H. Twizell, "The extrapolation of Padé approximants in the closed loop simulation of human thermoregulation", Accepted for publication in *Appl. Math. Modelling.*

11. Stolwijk, J.A.J., "Mathematical model of thermoregulation". In Hardy, J.D, et al (eds.), *Physiological and Behavioral Temperature Regulation,* Springfield, Illinois, C.C Thomas (Publisher), 1970 (Chapter 48, 703 - 721).

12. Stolwijk, J.A.J., and J.D. Hardy, "Temperature regulation in man : a theoretical study", *Pfuegers Arch.* 291 : 129 - 162, 1966.

13. Stolwijk, J.A.J. , and J.D. Hardy, in *Handbook of Physiology,* Bethesda, Maryland, American Physiological Society, 1977 (Chapter 4, section 9).

14. Thomas, N.T. , J. Spencer, and B.T. Davies, "A comparison of reactions to industrial protective clothing", *Ann. occup. Hyg,* 19 : 259 - 268, 1976.

15. Twizell, E.H. , and A .Q.M. Khaliq, "One—step multiderivative methods for first order ordinary differential euqations", Accepted for Publication in *BIT.*

16. Twizell, E.H. , and P. Smith, "Numerical modelling of heat flow in the human torso I : finite difference methods". Proceedings of *POLYMODEL 4 : Diffusion - Convection Problems,* Sunderland Polytechnic, May 1981.